‡*Department of Physiology and Biophysics, State University of New York, 124 Sherman Hall, Buffalo, New York 14214, USA*
e-mail: Sachs@buffalo.edu
†*Present address: Medizinische Klinik II, Universitaetsklinikum Luebeck, Ratzeburger Allee 160, 23538 Luebeck, Germany*

1. Ruknudin, A., Sachs, F. & Bustamante, J. O. *Am. J. Physiol.* **264,** H960–H972 (1993).
2. Hagiwara, N., Masuda, H., Shoda, M. & Irisawa, H. *J. Physiol. (Lond.)* **456,** 285–302 (1992).
3. Sato, R. & Koumi, S. *J. Membr. Biol.* **163,** 67–76 (1998).
4. Sachs, F. in *Cell Mechanics and Cellular Engineering* (eds Mow, V. C. *et al.*) 308–328 (Springer, New York, 1994).
5. Zabel, M., Koller, B. S., Sachs, F. & Franz, M. R. *Cardiovasc. Res.* **32,** 120–130 (1996).
6. Suchyna, T. M. *et al. J. Gen. Physiol.* **115,** 583–598 (2000).
7. Ravelli, F. & Allessie, M. *Circulation* **96,** 1686–1695 (1997).
8. Bode, F., Katchman, A., Woosley, R. L. & Franz, M. R. *Circulation* **101,** 2200–2205 (2000).
9. Caldwell, R. A., Clemo, H. F. & Baumgarten, C. M. *Am. J. Physiol.* **275,** C619–C621 (1998).
10. Small, D. L. & Morris, C. E. *Br. J. Pharmacol.* **114,** 180–186 (1995).
11. Kim, D. *J. Gen. Physiol.* **100,** 1021–1040 (1992).
12. Nazir, S. A. *et al. J. Physiol. (Lond.)* **494P,** 111–112 (1996).

Photonic engineering

Aphrodite's iridescence

The most intense colours displayed in nature result from either multilayer reflectors or linear diffraction gratings[1–3]. Here we investigate the spectacular iridescence of a spine (notoseta) from the sea mouse *Aphrodita* sp. (Polychaeta: Aphroditidae). The spine normally appears to be deep red in colour, but when light is incident perpendicular to the axis of the spine, different colours are seen as stripes running parallel to the axis of the spine; over a range of smaller incident angles, the complete visible spectrum is reflected with a reflectivity of 100% to the human eye. The simple structure responsible for this effect is a remarkable example of photonic engineering by a living organism.

Photonics is a branch of optics that concerns the control of photons, much as electronics depends on electrons, and photonic structures have been described in butterfly wings[4]. The sea mouse has iridescent spines situated at the base of the dorsal surface, where they can be viewed laterally, with less strongly coloured threads being seen more readily from above (see http://www.physics.usyd.edu.au/~nicolae/submitted.html). The biological function of the iridescence is unknown, but it may be related to species recognition or to courtship.

We prepared a spine with strong reflectance in the red for electron microscopy by mounting it in resin and slicing it with a microtome into sections transverse to the long axis. These sections were of constant thickness and were mounted on grids for transmission microscopy.

The micrograph in Fig. 1a shows an array of hollow cylinders, with the long axis of the cylinders along the spine. The image is of the wall region of the spine, the centre of the spine being hollow. The hollow cylinders have thicker walls near the edge of the spine, possibly for mechanical rigidity, but after a few layers their wall thickness decreases to a constant value. The cylinders are close-packed, with each cylinder having six nearest neighbours. The spacing of adjacent layers of cylinders is 0.51 μm, and remains constant throughout the wall cross-section, which contains 88 layers of close-packed voids. The cylinder walls are made of pure α-chitin[5,6] (refractive index, 1.54; ref. 2).

To calculate the expected optical properties of the spine, we used a formulation for layered stacks of cylinder gratings[7]. Figure 1c shows the reflectance of a 500-layer stack of gratings with period $d = 0.51$ μm, for radiation incident in the plane of Fig. 1a, with its electric vector perpendicular to the plane ($\mathbf{E}_{\|}$). The grating consists of hexagonally packed cylindrical holes of radius $a = 0.2$ μm, filled with sea water (refractive index, 1.33), in a matrix of chitin. The bulk reflectance of chitin immersed in sea water is 0.54%, so the strong reflectance evident in Fig. 1c can only be achieved through the coherent stacking of scores of layers to form the crystal shown in Fig. 1a. Were the layers to be of irregular separation or composition, the peak reflectance for a given number of layers would be much lower[7] and the iridescence less pronounced.

We calculated the total reflectance of this structure, for normal incidence, for free-space wavelengths in the visible spectrum (from 0.4 to 0.7 μm). Figure 1c shows a strong maximum in reflectance around the wavelength $\lambda = 0.633$ μm. To investigate the origin of this narrow-band reflectance, we calculated the photonic band diagram, which gives the frequencies

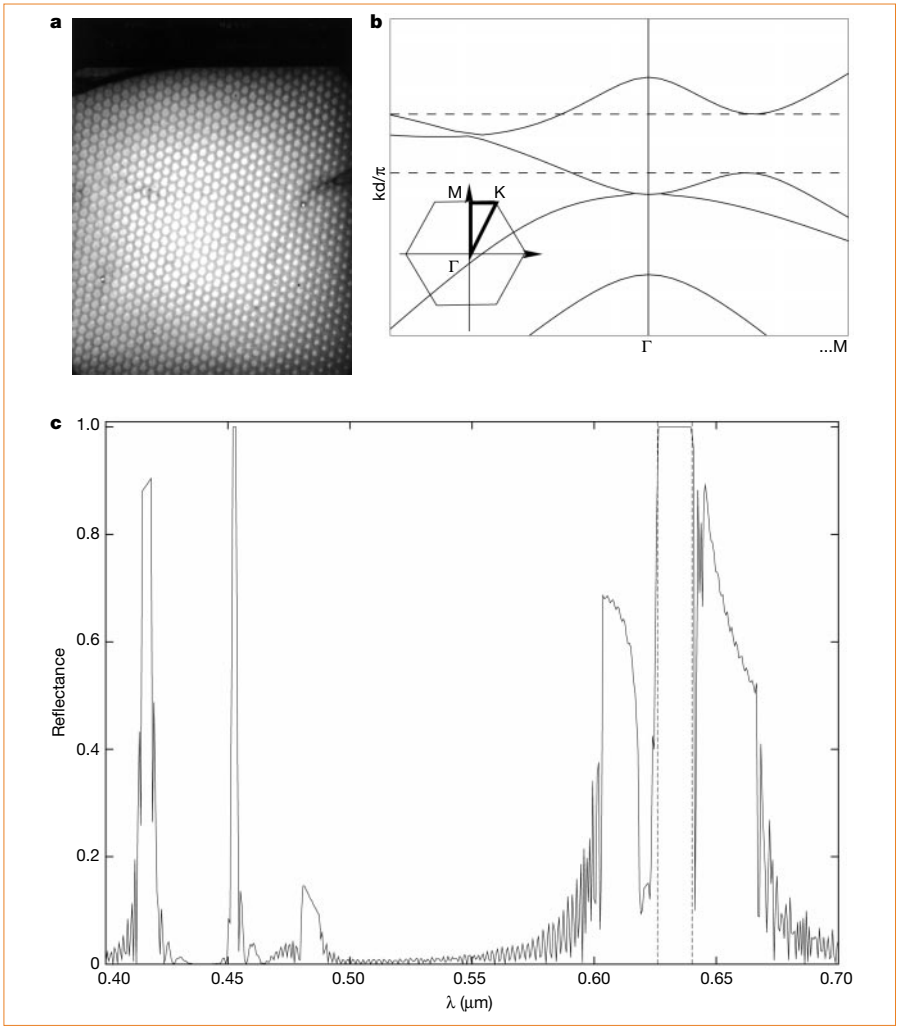

Figure 1 Structure and optical properties of a sea mouse hair from Palm Beach, New South Wales, Australia. **a,** Electron micrograph of a section of the spine (the dark regions are chitin). **b,** $\mathbf{E}_{\|}$ polarization photonic band structure for a hexagonal crystal of voids in chitin, near the four-fold degenerate point on the Γ-axis (dashed lines indicate a partial band gap). Γ, M and K are the corners of the irreducible part of the first Brillouin zone; k is the free space wavenumber. **c,** $\mathbf{E}_{\|}$ polarization total reflectance for normally incident radiation for a hexagonal structure having 500 layers of voids in chitin (dashed lines indicate the partial bandgap of **b**). Reflectance measurements using a Zeiss MMS spectrometer confirm a 100% reflectance in the red.

of light waves able to propagate freely in the structure, for the hexagonal array of voids (presumably water-filled) in a chitin matrix. This is shown in Fig. 1b for $\mathbf{E}_{||}$ polarization, indicating that the region of enhanced reflectance in the red for the spine corresponds exactly to a partial photonic bandgap of the hexagonal structure (in the range Γ–M) — a circumstance in which light cannot propagate in a narrow range of wavelengths in the structure. Note that for $\mathbf{H}_{||}$ polarization of incident radiation with the magnetic vector perpendicular to the plane of Fig. 1a, reflectance is similarly enhanced in the red, although there is not a clear-cut partial bandgap.

We have seen that the sea mouse achieves brilliant narrow-band coloration of its spines through a remarkable piece of photonic engineering. The regularity of the structure shown in Fig. 1a and the strong narrow-band reflectance shown in Fig. 1c suggest that growing optical filters by molecular self-assembly is a technological goal worth pursuing. These structures may have application in photonic communications, where there is much interest in fabricating photonic crystal fibres[8] with similar morphology to that shown in Fig. 1a in order to improve bandwidth and nonlinear properties.

Andrew R. Parker*, Ross C. McPhedran†, David R. McKenzie†, Lindsay C. Botten‡, Nicolae-Alexandru P. Nicorovici†

**Department of Zoology, University of Oxford, South Parks Road, Oxford OX1 3PS, UK*
†School of Physics, University of Sydney, New South Wales 2006, Australia
e-mail: ross@physics.usyd.edu.au
‡School of Mathematical Sciences, University of Technology, Sydney, New South Wales 2007, Australia

1. Parker, A. R. in *Functional Morphology of the Invertebrate Skeleton* (ed. Savazzi, E.) 65–90 (Wiley, Chichester, 1999).
2. Land, M. F. *Progr. Biophys. Mol. Biol.* **24,** 75–106 (1972).
3. Parker, A. R. *Proc. R. Soc. Lond. B* **262,** 349–355 (1995).
4. Vukusic, P. *et al. Proc. R. Soc. Lond. B* **266,** 1403–1411 (1999).
5. Rouse, G. in *Invertebrate Zoology* (ed. Anderson, D. T.) 174–203 (Oxford Univ. Press, Melbourne, 1998).
6. Atkins, E. D. T., Dlugosz, J. & Foord, S. *Int. J. Biol. Macromol.* **1,** 29–32 (1979).
7. McPhedran, R. C. *et al. Aust. J. Phys.* **52,** 791–809 (1999).
8. Knight, J. C. *et al. Science* **282,** 1476–1478 (1998).

Oceanography

Vertical mixing in the ocean

The thermohaline circulation of the ocean results primarily from downwelling at sites in the Nordic and Labrador Seas and upwelling throughout the rest of the ocean. The latter is often described as being due to breaking internal waves. Here we reconcile the difference between theoretical and observed estimates of vertical mixing in the deep ocean by presenting a revised view of the thermohaline circulation, which allows for additional upwelling in the Southern Ocean and the separation of the North Atlantic Deep Water cell from the Antarctic Bottom Water cell. The changes also mean that much less wind and tidal energy needs to be dissipated in the deep ocean than was originally thought.

Previous calculations of vertical mixing based on the stratification of the deep ocean[1,2] assumed that a flux of 25 or 30 sverdrups (Sv) of water, made up of both deep and bottom waters, is injected at depths of about 4,000 metres and mixed upwards to depths near 1,000 m by turbulent mixing. Both reports conclude that the spatially averaged diapycnal (cross-density surface) mixing coefficient is 10^{-4} m^2 s^{-1}.

However, observations of turbulence[3] and dye diffusion[4] in the deep ocean indicate that there exists a background diapycnal diffusivity of only 10^{-5} m^2 s^{-1}, although much larger values are found in localized regions near rough topography[5]. The background value is consistent with mixing due to the background internal wave field, and the larger values are consistent with extra internal waves due to the interaction of currents with topography.

But it is not obvious that the latter is enough to raise diffusivity by an order of magnitude when averaged over the whole ocean. The extra power required to do this is also large[6]. If the efficiency is 20%, which is normally considered a maximum for the final stage of breaking internal waves, then the power required is 2.1 terawatts. This is just possible, given current estimates of the energy input from the wind and tides, but this figure does not allow for losses at other stages in the conversion process.

A contrasting view of the thermohaline circulation has come from low-resolution[7] and high-resolution[8] computer model studies of the ocean circulation. These show that between 9 and 12 Sv of deep water is brought to the surface by Ekman suction in the Southern Ocean. This is driven northwards in the surface Ekman layer and is reduced in density primarily by surface freshening. The model results also emphasize earlier observations[9] that in the primary regions of bottom-water formation around Antarctica, the near-surface water masses have the same density as North Atlantic deep water. It is therefore not necessary for the bottom water to be mixed through the whole depth of the water column, only up to the level of the deep waters.

Using this new view of the thermohaline circulation, we need only consider the vertical mixing of the main deep-water mass, North Atlantic Deep Water, whose flux is estimated to lie between 14 and 17 Sv (ref. 10). Taking the larger of these two values and the smaller of the two model-based estimates of upwelling leaves a maximum of 8 Sv to be mixed vertically within the ocean. The 10^{-5} m^2 s^{-1} background term can upwell 3 Sv, leaving 5 Sv to be upwelled by localized regions of intense mixing. If this view is correct, then the vertical mixing coefficient, averaged over the whole ocean, is less than 3×10^{-5} m^2 s^{-1} and, assuming 20% efficiency, the total amount of extra energy required is less than 0.6 terawatts.

The revised values are consistent with existing observations of mixing within the ocean. They also emphasize again the importance of the Southern Ocean and imply that although further research is needed on the localized mixing in the deep ocean, such mixing does not control the thermohaline circulation.

D. J. Webb*, N. Suginohara†

**Southampton Oceanography Centre, Empress Dock, Southampton SO14 3ZH, UK*
e-mail: david.webb@soc.soton.ac.uk
†Center for Climate System Research, University of Tokyo, 4-6-1 Komaba, Meguro-ku, Tokyo 153-8904, Japan

1. Munk, W. H. *Deep-Sea Res.* **13,** 707–730 (1966).
2. Munk, W. H. & Wunsch, C. *Deep-Sea Res.* **45,** 1977–2010 (1998).
3. Gregg, M. C. *J. Geophys. Res.* **94,** 9686–9698 (1989).
4. Ledwell, J. R., Watson, A. J. & Law, C. S. *J. Geophys. Res.* **103,** 21499–21529 (1998).
5. Polzin, K. *et al. Science* **276,** 93–96 (1997).
6. Wunsch, C. *Nature* **405,** 743–744 (2000).
7. Toggweiler, J. R. & Samuels, B. *J. Phys. Oceanogr.* **28,** 1832–1852 (1998).
8. Döös, K. & Coward, A. C. *Int. WOCE Newslett.* **27,** 3–4 (1997).
9. Foster, T. D. & Carmack, E. C. *Deep-Sea Res.* **23,** 301–317 (1976).
10. Schmitz, W. J. *Rev. Geophys.* **33,** 151–173 (1995).

Antibiotic resistance

How wild are wild mammals?

In bacteria associated with humans, antimicrobial resistance is common, both in clinical isolates and in the less-studied commensal flora, and it is thought that commensal and environmental bacteria might be a hidden reservoir of resistance. Gilliver *et al.* have reported that resistance is also prevalent in faecal bacteria from wild rodents living in northwest England[1]. Here we test the faeces of moose, deer and vole in Finland and find an almost complete absence of resistance in enterobacteria. Resistance is thus not a universal property of enterobacterial populations, but may be a result of the human use of antibiotics.

Bacterial resistance to antimicrobial agents has become a serious problem in modern medicine and a debated evolutionary question[2]. The use — and misuse — of antibiotics is generally blamed, but it has also been claimed that there must be other reasons for the increase in resistance[3]. This question is important: if resistance increases independently of antibiotic use, restrictive policies would be unnecessary. One way to test the effect of human activities is to compare the resistance frequencies of popula-